



## Short range order in Al–Fe–Nb, Al–Fe–Ce and Al–Ni–Ce metallic glasses

F. Saporiti<sup>a,\*</sup>, M. Boudard<sup>b,c</sup>, F. Audebert<sup>a</sup>

<sup>a</sup> Grupo de Materiales Avanzados, Facultad de Ingeniería, Universidad de Buenos Aires, Paseo Colón 850 (C1063ACV) Buenos Aires, Argentina

<sup>b</sup> LMGP, MINATEC Bâtiment INPG, UMR 5628 CNRS-INPG, 3 parvis Louis, Néel, BP 257, 38016 Grenoble France

<sup>c</sup> SIMAP-ENSEEG, UMR 5614 CNRS-INPG-UJF, BP75, 38402 St Martin d'Hères, France

### ARTICLE INFO

#### Article history:

Received 31 July 2008

Received in revised form

24 November 2009

Accepted 1 December 2009

Available online 6 December 2009

#### Keywords:

Amorphous

X-ray diffraction

Structure

Local order

### ABSTRACT

Short range order of amorphous samples with Al<sub>90</sub>Fe<sub>7</sub>Nb<sub>3</sub>, Al<sub>90</sub>Fe<sub>5</sub>Ce<sub>5</sub> and Al<sub>90</sub>Ni<sub>5</sub>Ce<sub>5</sub> nominal composition (in at.%) was studied by X-ray diffraction (XRD) at room temperature (RT). The total structure factors  $S_{\text{Tot}}(Q)$  and the reduced atomic distribution function  $G(r)$  were derived from the diffracted intensity  $I_M(Q)$ . All the  $S_{\text{Tot}}(Q)$  factors are composed by an initial prepeak followed by a main peak and a second peak with two components. Though the general aspect of the different samples is similar they present slight differences in details that are discussed as a function of the composition and compared with available data in the literature. While in the Al–(Fe, Ni)–Ce alloys two distinct components were observed for the first peak of the  $G(r)$  function, a unique broad peak was observed in the Nb containing alloy. The pair correlation function,  $g(r)$ , for Al<sub>90</sub>Fe<sub>10</sub> at 200 K have been calculated with molecular dynamics simulation (MDS) and it is in good agreement with the experimental results obtained from Al<sub>90</sub>Fe<sub>7</sub>Nb<sub>3</sub> showing that size effects can be neglected in this sample.

© 2010 Elsevier B.V. All rights reserved.

### 1. Introduction

Al-based amorphous and partially crystallized alloys have been widely studied due to the possibility of developing light alloys with high strength with good ductility or toughness [1]. Our interest deals with ternary samples obtained by addition of relatively small quantities of Ce to both Al–Fe and Al–Ni alloys, and of Nb to an Al–Fe alloy. At least two characteristics related to these alloys have been considered in the present study. One characteristic is related to the effect of the transition metals (TM) in the solid and liquid Al-based systems, which have different local order depending on the TM contained in the alloy (mainly tetrahedral and icosahedral orders), as was previously reported [2–8]. Medium short range order is present in these alloys and was related to a strong heteroatomic interaction which can be related to a certain covalent character of the atomic bonds (which should be varying according to the TM electronic structure). The other characteristic is related to the effect of the rare earth (RE) atoms, on Al–RE and Al–TM–RE metallic glasses with a high Al content (up to 90 at.%) [9–11]. The large difference of the size of the atoms in the alloy leads to a topological order with a high packing fraction. Amorphous models were built based on a cluster with a central RE atom surrounded by essentially Al atoms [12]. A more complicated scenario is expected when complex interaction between the three components of the alloys exists.

In this work, a comparative study of the short range order of amorphous samples with Al<sub>90</sub>Fe<sub>7</sub>Nb<sub>3</sub>, Al<sub>90</sub>Fe<sub>5</sub>Ce<sub>5</sub> and Al<sub>90</sub>Ni<sub>5</sub>Ce<sub>5</sub> nominal composition (in at.%) is presented. The particular composition of these alloys may help in the understanding of the different origin of local order which have been considered (topological order and chemical interaction). The different TM (Fe or Ni) in the ternary samples with Ce is sensitive to a difference in the Al–TM chemical interaction. Comparison of Al<sub>90</sub>Fe<sub>7</sub>Nb<sub>3</sub><sup>1</sup> and Al<sub>90</sub>Fe<sub>5</sub>Ce<sub>5</sub> alloys is sensitive to different topological effect (Nb alloys have not much size effect whereas Ce alloys do). Besides classical extraction of the reduced atomic distribution function  $G(r)$  from the experimental X-ray diffraction (XRD) data a molecular dynamic simulation (MDS) was carried out on pure and binary alloys which can help in the understanding of the glass forming ability of amorphous Al-based alloys.

### 2. Experimental procedures, analysis of the data and MDS conditions

Ingots with starting nominal composition Al<sub>90</sub>Fe<sub>5</sub>Ce<sub>5</sub>, Al<sub>90</sub>Ni<sub>5</sub>Ce<sub>5</sub> and Al<sub>90</sub>Fe<sub>7</sub>Nb<sub>3</sub> were prepared from high purity elements (Al, Fe, Ni and Ce with 99.99% and Nb with 99.7%).

<sup>1</sup> The Al–Fe–Nb alloy composition was chosen to obtain a completely amorphous sample as reported in the work of Audebert et al [13]. As far as size effect is concerned the Al<sub>90</sub>Fe<sub>7</sub>Nb<sub>3</sub> behaves as a hypothetical Al<sub>90</sub>Fe<sub>10</sub> sample as it is shown by the molecular dynamic simulation (MDS). Thus the comparative study of Al<sub>90</sub>Fe<sub>7</sub>Nb<sub>3</sub> with Al<sub>90</sub>Fe<sub>5</sub>Ce<sub>5</sub> remains of interest.

\* Corresponding author. Tel.: +54 11 4343 0891x381.

E-mail address: [fsapori@fi.uba.ar](mailto:fsapori@fi.uba.ar) (F. Saporiti).

$\text{Al}_{90}\text{Fe}_5\text{Ce}_5$  and  $\text{Al}_{90}\text{Ni}_5\text{Ce}_5$  amorphous ribbons were obtained from the pre-alloyed ingot by the melt-spinning technique under a partial helium atmosphere. The ribbons obtained have typical dimensions of 15–25 microns thick, 1–3 mm wide.  $\text{Al}_{90}\text{Fe}_7\text{Nb}_3$  amorphous ribbons were obtained by planar flow casting under air atmosphere with typical dimensions of 15–25 microns thick, 8–10 mm wide<sup>2</sup>. XRD studies data were performed in transmission geometry at RT using a Nonius Kappa CCD diffractometer (ENRAF Nonius Fr 590). The Mo-K $\alpha$  radiation (0.7071 Å) from a sealed tube was selected with a graphite monochromator. Diffraction data were collected with the CCD detector with a maximum value of  $Q = 4\pi \sin \theta / \lambda = 15 \text{ \AA}^{-1}$ . For each sample, a background image was collected in exactly the same conditions and subtracted from sample images. The total diffracted intensity measured ( $I_M(Q)$  vs.  $Q$ ) was obtained considering a narrow central strip of the two-dimensional image from the CCD detector and applying polarization and absorption correction.  $I_M(Q)$  data were subsequently corrected from inelastic scattering (Compton and fluorescence) and normalized (using PDFgetX2 software [14]) to obtain the total elastic scattering intensity per atom ( $I_{\text{e.u.}}^{\text{coh}}(Q)$  in electron units), that was used to calculate the total structure factor in the Faber Zimman formalism ( $S_{\text{Tot}}(Q)$ ) according to Eq. (1):

$$S_{\text{Tot}}(Q) = \frac{I_{\text{e.u.}}^{\text{coh}}(Q) - [\langle f^2(Q) \rangle - \langle f(Q) \rangle^2]}{\langle f(Q) \rangle^2} \quad (1)$$

The reduced atomic distribution function,  $G(r)$ , was obtained by Fourier transform according to Eq. (2):

$$G(r) = \frac{2}{\pi} \int_0^{Q_{\text{max}}} Q[S(Q) - 1] \sin(Qr) dQ \quad (2)$$

The  $G(r)$  functions were calculated with truncation values  $Q_{\text{max}}$  equal to  $13 \text{ \AA}^{-1}$  when applying Eq. (2).

A MDS has been performed at different temperatures to study the structure of liquid and amorphous states of pure Al, Fe and binary  $\text{Al}_{90}\text{Fe}_{10}$  and  $\text{Al}_{90}\text{Ni}_{10}$  alloys. The interaction between atoms has been modeled applying the embedded atom method developed by Daw and Baskes [15]. The simulation was performed following the method used in an early work [16], using a microcanonical ensemble (NVE), where  $N$  is the number of atoms ( $N = 1372$  atoms),  $V$  the volume and  $E$  the total energy of the system,  $N$  and  $E$  were kept constant. The pair correlation function,  $g(r)$ , obtained from MDS has been used to describe the structure of the amorphous state of Al, Fe and  $\text{Al}_{90}\text{Fe}_{10}$  and  $\text{Al}_{90}\text{Ni}_{10}$  alloys. The reduced atomic distribution function,  $G(r)$ , is related to  $g(r)$  through the density of the sample  $\rho_0$  by Eq. (3):

$$G(r) = 4\pi\rho_0(g(r) - 1) \quad (3)$$

### 3. Results and discussion

The results will be presented and discussed first in the reciprocal space. A description of the total structure factors is given and compared with the results present in the literature followed by a detailed discussion of the prepeak. In a second stage, a description and discussion of the experimental reduced atomic distribution function that is finally compared with MDS results is presented.

The total structure factors  $S_{\text{Tot}}(Q)$  (Fig. 1) have the same general features characterized by a prepeak near  $Q = 1.4 \text{ \AA}^{-1}$ , a main first peak around  $3 \text{ \AA}^{-1}$ , a subsequent second peak with a clear splitting and finally a third peak. The fourth and fifth contributions at higher

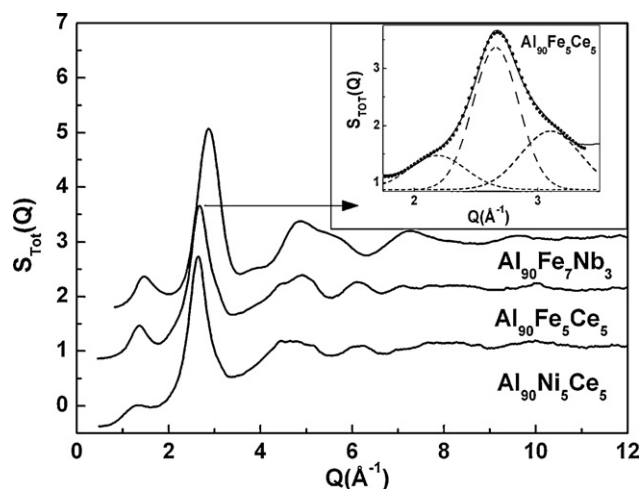


Fig. 1. Total structure factors  $S_{\text{Tot}}(Q)$  obtained from XRD experiments for the different samples. The inset presents an example ( $\text{Al}_{90}\text{Fe}_5\text{Ce}_5$  alloy) of decomposition of the main peak considering three Gaussian components (dashed line). Their sum (dotted line) reproduces satisfactorily the experimental data (continuous line).

$Q$  are more or less clearly seen depending on the sample. Close inspection of Fig. 1 shows that the structure factors differ however in details:

- Those of Al–(Ni, Fe)–Ce alloys presents a general shift at smaller  $Q$  values with respect to the one of Al–Fe–Nb sample. This observation can be related to the large atomic radius of Ce that leads to an increase of the average interatomic distances (corresponding to a shift at smaller  $Q$  values in the reciprocal space).
- The main peak is intense and broad for the Al–Fe–Nb alloy with a unique component at  $2.85 \text{ \AA}^{-1}$ , whereas in Al–(Ni, Fe)–Ce this main peak results from the superposition of three peaks: an intense narrow main component is present around  $2.65 \text{ \AA}^{-1}$  with two additional minor contributions on both sides of this peak (see the inset of Fig. 1).
- The prepeak of the Al–Ni–Ce alloys has less intensity than those corresponding to Al–Fe–(Ce or Nb) alloys. Since the prepeak is related to clusters formed with a strong interaction between unlike atoms, the Ni containing alloy would have a more homogeneous amorphous structure than the Fe containing alloys [7].

The results obtained in the present work agree with previous results on the total structure factor  $S_{\text{Tot}}(Q)$  obtained on  $\text{Al}_{90}\text{Fe}_5\text{Ce}_5$  [17,18],  $\text{Al}_{85}\text{Ni}_{10}\text{Ce}_5$  [19,20]<sup>3</sup> and in  $\text{Al}_{90}\text{Ni}_5\text{Ce}_5$  samples [20]. Similar XRD results were also obtained by Zhang et al. [6] that compare Al–Fe and Al–Fe–Ce samples both in liquid and amorphous solid at different temperatures. They showed that the prepeak present in the liquid is retained in the amorphous phase and the first peak of  $S_{\text{Tot}}(Q)$  shows a complex structure with several components and a splitting on the second peak contribution. The first peak in the  $S_{\text{Tot}}(Q)$  of the liquid Al–Fe–Ce is broaden with respect to liquid Al–Fe. In Al–Ni–Nd samples studied by neutron diffraction [21], the  $S_{\text{Tot}}(Q)$  function has a prepeak near  $1.5 \text{ \AA}^{-1}$  and a main peak asymmetric with two contribution near  $2.66 \text{ \AA}^{-1}$  and  $3.06 \text{ \AA}^{-1}$  that agree with our results. Similar behavior was also found for Al–(Fe–Ni)–Si amorphous samples [2,3] though the less pronounced asymmetry of the main peak reported when Fe is replaced by Ni in that amorphous  $S_{\text{Tot}}(Q)$  is not observed in Al–(Fe/Ni)–(Ce/Nb) samples in the

<sup>2</sup> Both techniques used for obtaining amorphous samples in our experiments give essentially the same results as far as the thicknesses of the samples are similar.

<sup>3</sup> The results presented in Fig. 1 can be compared with Fig. 1 of [18] and with Fig. 1 of [19] (the splitting of the first peak is more pronounced for this  $\text{Al}_{85}\text{Ni}_{10}\text{Ce}_5$  composition). The prepeaks are not shown in [20].

present work. It is worth noting that, recently, close results to ours were obtained also on  $\text{Al}_{89}\text{Ni}_5\text{La}_6$  amorphous sample [22] which was obtained on the base of the  $\text{Al}_{86}\text{Ni}_8\text{Y}_6$  alloy [23].

Discussing in more detailed about the prepeak position, it is observed that the value obtained for Ce containing alloys in the present work ( $1.34\text{--}1.36\text{ \AA}^{-1}$ ) compares fairly well with those obtained by other authors:  $1.38\text{ \AA}^{-1}$  in [6]<sup>4</sup>,  $1.32\text{ \AA}^{-1}$  in [18] ( $\text{Al}_{90}\text{Fe}_5\text{Ce}_5$  sample) and near  $1.35\text{ \AA}^{-1}$  in [19] ( $\text{Al}_{85}\text{Ni}_{10}\text{Ce}_5$  sample). Those values are intermediate between the value for binary Al–Fe ( $1.60\text{ \AA}^{-1}$  [6]) and Al–RE alloys ( $1.23\text{ \AA}^{-1}$  obtained by extrapolation for Al–Ce [18] and  $1.3\text{ \AA}^{-1}$  for  $\text{Al}_{90}\text{Y}_{10}$  and  $\text{Al}_{87}\text{Ni}_7\text{Y}_5$  alloys [10]).

Two different mechanisms appear to be related to Al–TM and Al–Re interactions:

- Al–TM interactions can be discussed with reference to the work by Maret et al. [4] and Zhang et al. [6] on Al–TM binary liquid alloys.  $\text{Al}_{80}\text{Ni}_{20}$  and  $\text{Al}_{80}\text{Mn}_{20}$  liquids show the existence of a prepeak (around  $1.8\text{ \AA}^{-1}$ ) in the total structure factor due to superstructure effects resulting from heteroatomic interactions between Al and TM with weak correlation lengths ( $4\text{ \AA}$ ). The possible contribution to the prepeak due to size effect is negligible in these systems. Al–Ni is less ordered with respect to Al–Mn and presents a different local order.
- Hsieh et al. [18] discussed experimental XRD results from amorphous structure in the Al–Fe–Ce alloys with respect to the one obtained from dense random packing (DRP) model. They considered a binary alloy system in which the minority atoms B are repelling each other but more or less uniformly distributed and calculated with a DRP model the resulting prepeak position for an  $\text{Al}_{90}\text{Fe}_{10}$  system ( $1.28\text{ \AA}^{-1}$ ) and for an  $\text{Al}_{90}\text{Ce}_{10}$  system ( $1.23\text{ \AA}^{-1}$ ). These results show that only Al–RE contribution can be satisfactorily simulated through a DRP model and could thus be due to size effect.

In the present work, the position of the prepeak varies with Ce and Nb (near  $1.36\text{ \AA}^{-1}$  for Ce containing alloys and  $1.45\text{ \AA}^{-1}$  in the case of Nb). These observations are compatible with a scenario where heterochemical interactions with almost no size effects (Fe, Nb and Al have similar radius) are dominant in the Nb alloys (and probably dominated by Al–Fe interaction as there is a low content in Nb) whereas size effects are important in Ce containing alloys.

The structural unit size involved (estimated according to  $2\pi/Q_p$ , where  $Q_p$  is the position of the prepeak) are between  $4.3\text{ \AA}$  and  $4.7\text{ \AA}$  with correlation length (estimated as  $2\pi/\Delta Q_p$  where  $\Delta Q_p$  is the half-width of the prepeak) of  $12\text{ \AA}$  in the Nb containing alloy and between  $15\text{ \AA}$  and  $25\text{ \AA}$  in containing Ce alloys (relatively large when compared with those present in liquid alloys ( $9\text{ \AA}$ ), [24]). A slightly larger cluster size (equivalent to the correlation length of the heteroatomic units) as well as a larger area of the prepeak in Ce containing alloys with Fe content when compared with those with Ni content could be an indication of a different structure of  $\text{Al}_{90}\text{Fe}_5\text{Ce}_5$  and  $\text{Al}_{90}\text{Ni}_5\text{Ce}_5$  amorphous samples though the structure factors appear to be close to each other. In particular a difference is expected from previous results which show a different local order for  $\text{Al}_{80}\text{Ni}_{20}$  alloys (tetrahedral) as compared with

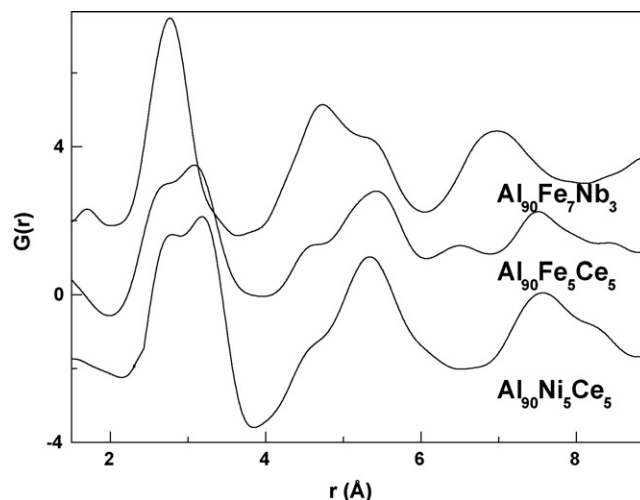


Fig. 2. Experimental reduced atomic distribution function,  $G(r)$ , for amorphous  $\text{Al}_{90}\text{Fe}_7\text{Nb}_3$ ,  $\text{Al}_{90}\text{Fe}_5\text{Ce}_5$  and  $\text{Al}_{90}\text{Ni}_5\text{Ce}_5$ .

$\text{Al}_{80}\text{Fe}_{20}$  alloys (icosahedral)<sup>5</sup>. Similar results to ours and in particular a larger area of the prepeak in  $\text{Al}_{90}\text{Fe}_5\text{Ce}_5$  alloy than the one in  $\text{Al}_{90}\text{Ni}_5\text{Ce}_5$  alloy is also shown in [25]. Moreover, they found that when annealing is performed at a temperature just above the onset of crystallization, the prepeak still exists for the  $\text{Al}_{90}\text{Fe}_5\text{Ce}_5$  amorphous alloy, whereas the prepeak disappears for the  $\text{Al}_{90}\text{Ni}_5\text{Ce}_5$  amorphous alloy [25].

Fig. 2 represents the reduced atomic distribution function,  $G(r)$ , and Table 1 summarizes the positions of the maxima of this function obtained from a multi-components Gaussian fit. First peak in Fig. 2 contains contributions due to the first neighbors. It has essentially three contributions from Al–Al pair expected (from the value of the metallic radius) at  $2.86\text{ \AA}$ , Al–(Fe or Ni) expected around  $2.68\text{ \AA}$  and Al–Ce (resp. Al–Nb) expected at  $3.24\text{ \AA}$  (resp.  $2.89\text{ \AA}$ ). The bonds contributing to the main peak in the Nb containing alloy have very similar length and result in a broad peak centered experimentally at  $2.76\text{ \AA}$  (peak 1 in Table 1).

For Al–(Fe, Ni)–Ce samples the fit of the first peak in Fig. 2 gives two Gaussian contributions (marked peak 1 and 2 in Table 1) with a clearly splitting due to the long Al–Ce (peak 2) bond resulting from the large value of Ce metallic radius. A more detailed analyses<sup>6</sup> with three components (not shown in Table 1) corresponding to Al–TM, Al–Al and Al–Ce distances leads to  $2.45\text{ \AA}$ ,  $2.68\text{ \AA}$  and  $3.15\text{ \AA}$  for the Al–Fe–Ce alloy and  $2.47\text{ \AA}$ ,  $2.78\text{ \AA}$  and  $3.25\text{ \AA}$  for the Al–Ni–Ce alloy which are close to each other (Al–TM and Al–Ce distances appears slightly larger for Al–Ni–Ce alloys). These results agree with [18,19]. The most important difference when compared to Al–Fe–Nb alloy is the distinct contribution near  $3.2\text{ \AA}$ . Results found in the literature by different techniques (e.g. XRD [19], EXAFS [26] and XANES [27]) gave the same tendency as our results with a first coordination shell build of Al–TM, Al–Al and Al–Ce bonds (by example in reference [19] distances are close to  $2.5\text{ \AA}$  (Al–Ni),  $2.75\text{ \AA}$  (Al–Al) and  $2.9\text{ \AA}$  –  $3.2\text{ \AA}$  (Al–Ce)). Even though a difference is expected for Fe and Ni containing alloys and which in turn could be related to different intermediate distance Al–Fe and Al–Ni, no clear difference between Al–Ni–Ce and Al–Fe–Ce alloys is observed in our samples.

Fig. 3 shows the pair correlation functions,  $g(r)$ , at 200 K obtained by MDS for pure Al and Fe and for the binary  $\text{Al}_{90}\text{Fe}_{10}$  at 200 K. These

<sup>4</sup> Al–Fe–Ce and Al–Fe samples in liquid and solid amorphous have been studied. Prepeak for Al–Fe is found at  $1.58\text{ \AA}^{-1}$ . Prepeaks in both samples remain in the liquid state up to  $1550\text{ }^\circ\text{C}$  although their intensities and that of the main peak decrease with increasing temperature as expected for greater disorder but position remains mostly unchanged.

<sup>5</sup> A quasiperiodic icosahedral phase is observed in Al–Fe–Ce system but this is not the case in Al–Ni based system though quasiperiodic decagonal phases are observed.

<sup>6</sup> The individual contributions (Al–Al and Al–TM) are not easily resolved because both the atomic radii and the X-ray form factors of Al and TM atoms are close to each other.

**Table 1**  
Positions of the Gaussian peaks used to adjust the function  $G(r)$  in Fig. 2. The peaks positions and estimated errors are in Å.

| Sample   |  | Peak position |             |             |             |             |             |             |
|--|--|---------------|-------------|-------------|-------------|-------------|-------------|-------------|
|  |  | 1             | 2           | 3           | 4           | 5           | 6           | 7           |
| Al <sub>90</sub> Fe <sub>5</sub> Nb <sub>5</sub> |  | 2.76 ± 0.03   |             | 4.7 ± 0.06  | 5.46 ± 0.06 |             | 6.73 ± 0.06 | 7.23 ± 0.08 |
| Al <sub>90</sub> Fe <sub>5</sub> Ce <sub>5</sub> |  | 2.80 ± 0.03   | 3.25 ± 0.06 | 4.53 ± 0.06 | 5.36 ± 0.06 | 6.59 ± 0.06 |             |             |
| Al <sub>90</sub> Ni <sub>5</sub> Ce <sub>5</sub> |  | 2.89 ± 0.03   | 3.28 ± 0.06 | 4.55 ± 0.06 | 5.33 ± 0.06 | 6.11 ± 0.06 | 6.7 ± 0.06  | 7.41 ± 0.08 |

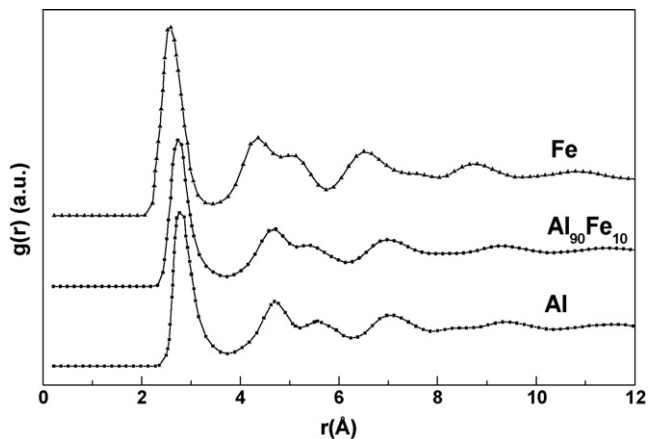


**Fig. 3.** Pair correlation function,  $g(r)$ , at 200 K from MDS for pure Al, Fe and Al<sub>90</sub>Fe<sub>10</sub> alloy.

functions show typical characteristics of amorphous samples with a main peak and a second peak that is splitted into two subpeaks. The position of the peaks shifts towards smaller  $r$  values when Al is substituted by Fe in agreement with a larger atomic radius of Al respect to Fe, leading to a shorter average interatomic distance. The pair correlation function obtained by MDS for Al<sub>90</sub>Fe<sub>10</sub> at 200 K fits with very good agreement the experimental curve of Al<sub>90</sub>Fe<sub>7</sub>Nb<sub>3</sub> sample represented in Fig. 2. The agreement with the experimental curves of Al–(Fe, Ni)–Ce is not so good due to the presence of Ce atoms which are not taken into account in the binary Al<sub>90</sub>Fe<sub>10</sub> obtained by MDS. In particular the first peak has a width greater than the MDS curve that can directly be explained by the long Al–Ce distances (see Fig. 2).

#### 4. Conclusions

The pair distribution function obtained from XRD experiments of Al<sub>90</sub>Fe<sub>7</sub>Nb<sub>3</sub> sample can be well explained by MDS considering a binary Al<sub>90</sub>Fe<sub>10</sub> alloy.

Differences in the pair distribution function obtained by MDS and XRD for Al<sub>90</sub>(Fe or Ni)<sub>5</sub>Ce<sub>5</sub> samples appear to be related to an important topological (size) effect present in these samples. From the experimental results it can be concluded that no difference in the main and second peak is observed for Ce containing samples irrespectively of the TM (Fe or Ni), which suggests that both alloys

have similar local order dominated by topological (size) effects related to different size of atoms. However, a slight difference is observed in the amorphous structure of these alloys since larger heteroatomic clusters are observed for the alloy that contains Fe than for the one with Ni.

The structural unit size of Ce containing alloys is bigger than in the Nb containing alloy, which can be related to the larger size of Ce atoms. Due to the fact that the correlation length is larger for the alloys with Ce than for the one with Nb, it can be concluded that Ce increases the medium range order.

#### References

- [1] A. Inoue, *Prog. Mater. Sci.* 43 (1998) 365.
- [2] B. Chenal, Thesis, University of Nancy, INPL France, 1988.
- [3] J.M. Dubois, Ch. Janot, *J. Phys.* 48 (1987) 1981.
- [4] M. Maret, T. Pomme, A. Pasturel, P. Chieux, *Phys. Rev. B* 42 (1990) 1598.
- [5] N. Jakse, O. Lebacqz, A. Pasturel, *Phys. Rev. Lett.* 90 (2004) 207801.
- [6] L. Zhang, Y. Wu, X. Bian, H. Lui, W. Wang, S. Wu, *J. Non-Cryst. Solids* 262 (2000) 169.
- [7] F. Audebert, C. Mendive, A. Vidal, *Mater. Sci. Eng. A* 375–377 (2004) 1196.
- [8] F. Audebert, in: B. Idzikowski, P. Švec, M. Miglierini (Eds.), *Properties and applications of nano-crystalline alloys from amorphous precursors series*, NATO Science Series II: Mathematics Physics and Chemistry, vol.184, Kluwer Academic Publishers, Dordrecht, 2005, p. 301.
- [9] A. Inoue, K. Ohtera, T. Masumoto, *Jpn. J. Appl. Phys.* 27 (1988) L1796.
- [10] E. Matsubara, Y. Waseda, A. Inoue, K. Ohtera, T. Masumoto, *Z. Naturforsch.* 44a (1989) 814.
- [11] A. Inoue, T. Zhang, K. Kita, T. Masumoto, *Mater. Trans. JIM* 30 (1988) 870.
- [12] D.B. Miracle, O.N. Senkov, *J. Non-Cryst. Solids* 319 (2003) 174.
- [13] F. Audebert, H. Sirkin, A. Garcia Escorial, *Phil. Mag. B* 76 (4) (1997) 483.
- [14] X. Qiu, J.W. Thomson, S.J.L. Billinge, *J. Appl. Crystallogr.* 37 (2004) 678.
- [15] M.S. Daw, M.L. Baskes, *Phys. Rev. B* 29 (1984) 6443.
- [16] F. Saporiti, F. Audebert, S. Gabbanelli, *J. Metastable Nanocryst. Mater.* 20–21 (2004) 629.
- [17] H.Y. Hsieh, B.H. Toby, T. Egami, Y. He, S.J. Poon, G.J. Shiet, *J. Mater. Res.* 5 (1990) 2807.
- [18] H.Y. Hsieh, T. Egami, Y. He, S.J. Poon, G.J. Shiet, *J. Non-Cryst. Solids* 135 (1991) 248.
- [19] O.P. Rachek, *J. Non-Cryst. Solids* 352 (2006) 3781.
- [20] C. Triveño Rios, S. Suriñach, M.D. Baró, C. Bolfarini, W.J. Botta, C.S. Kiminami, *J. Non-Cryst. Solids* 354 (2008) 4874.
- [21] K. Ahn, D. Louca, S.J. Poon, G.J. Shiet, *Phys. Rev. B* 70 (2004) 224103.
- [22] H.W. Sheng, Y.Q. Cheng, P.L. Lee, S.D. Shastri, E. Ma, *Acta Mater.* 56 (2008) 6264.
- [23] B.J. Yang, J.H. Yao, J. Zhang, H.W. Yang, J.Q. Wang, E. Ma, *Scripta Mater.* 61 (2009) 423.
- [24] Z. Fang, W. Youshi, Z. Chuanjiang, Z. Zhiqian, S. YuanChang, Z. Guorong, *J. Phys. Condens. Matter* 14 (2002) 1163.
- [25] Z. Fang, W. Youshi, S. YuanChang, Z. Chuanjiang, Z. Zhiqian, *Mater. Sci. Eng. A340* (2003) 212.
- [26] T.I. Sevastyanova, G.E. Yalovega, A. Mansour, A. Marchelli, A.V. Soldatov, *Phys. Solid State* 43 (2001) 961.
- [27] A.N. Mansour, A. Marcelli, G. Cibin, G.E. Yalovega, T.I. Sevastyanova, A.V. Soldatov, *Phys. Rev. B* 65 (2002) 134207.